construction materials

MDPI

Article

Assessment of Post-Tensioned Grout Durability by Accelerated Robustness and Corrosion Testing

Samanbar Permeh and Kingsley Lau *

Department of Civil and Environmental Engineering, Florida International University, Miami, FL 33174, USA; samanbar.permeh1@fiu.edu
* Correspondence: kilau@fiu.edu

Abstract: The corrosion of steel in post-tensioned tendons has been associated with deficient grout materials containing high free sulfate ion concentrations. In a Florida bridge in 2011, tendon corrosion failures occurred for a prepackaged thixotropic grout that had developed material segregation. However, the available grout and corrosion testing prescribed in material specifications, such as grout bleed water testing, was not able to identify the propensity or modality for the grout deficiencies and the associated steel corrosion that was observed in the field. It was of interest to identify corrosion testing methods that could prescribe grout resistance to segregation-related deficiencies that can form by aberrations in construction. The objectives of the work presented here included (1) characterizing the development of physical and chemical grout deficiencies due to excess mix water and water volume displacement, (2) developing small scale test methodologies that identify deficient grout, and (3) developing test methodologies to identify steel corrosion in deficient grout. The inverted-tee test (INT) and a modified incline-tube (MIT) test were assessed and both were shown to be useful to identify the robustness of grout materials to adverse mixing conditions (such as overwatering and pre-hydration) by parameters such as sulfate content, moisture content, electrical resistance, and steel corrosion behavior. It was shown that the different grout products have widely different propensities for segregation and accumulation of sulfate ions but adverse grout mixing practices promoted the development of grout deficiencies, including the accumulation of sulfate ions. Corrosion potentials of steel < −300 mV_{CSE} developed in the deficient grout with higher sulfate concentrations. Likewise, the corrosion current density showed generally high values of >0.1 $\mu A/cm^2$ in the deficient grouts. The values produced from the test program here were consistent with historical data from earlier research that indicated corrosion conditions of steel in deficient grout with >0.7 mg/g sulfate, further verifying the adverse effects of elevated sulfate ion concentrations in the segregated grout.

Keywords: corrosion; post-tensioned (PT); grout; accelerated testing

Citation: Permeh, S.; Lau, K. Assessment of Post-Tensioned Grout Durability by Accelerated Robustness and Corrosion Testing. *Constr. Mater.* **2023**, *3*, 449–461. https://doi.org/10.3390/constrmater3040029

Received: 27 September 2023
Revised: 30 October 2023
Accepted: 17 November 2023
Published: 23 November 2023

1. Introduction

Prestressed concrete by post-tensioning (PT) methods has been widely used for bridge construction, providing greater range of design possibilities and positive material and construction characteristics to improve durability. Cementitious grout in bonded PT systems provides barrier protection from the external environment in addition to protection afforded by the concrete element and the tendon duct material [1–3]. As the grout is typically made from Portland cement, the steel strand is further protected from corrosion by the development of a passive layer due to the alkaline grout pore water solution. These corrosion protection levels are often effective in preventing corrosion of the embedded steel; however, there have been several cases of premature corrosion in Florida bridges and elsewhere [4–8]. Many of those cases were related to the inadequate or degraded protection of the strand at joints where moisture and chloride ions can penetrate. Other cases were related to the development of void spaces within the tendon due to the formation of bleed water. In those instances, the steel strand was partially exposed in the grout voids in contact

with the bleed water lens. In part due to aggregation of chloride ions by the transport of the bleed water, as well as possible carbonation and moisture recharge due to imperfect duct sealing, macrocell coupling of the developed corrosion anodes at the grout–air interface and the remaining steel (strand embedded in the grout and auxiliary steel components) resulted in accelerated corrosion. Material specifications since the early 2000s for grout with non-bleed characteristics were established to prevent the corrosion associated with grout bleed water; however, by 2011, there were cases where steel strand corrosion developed in grouts meeting the non-bleed thixotropic grout specifications [9–14]. The corrosion was not associated with bleed water or void formation and chloride ion concentrations were not significantly elevated in those cases. Some of these cases were associated with physically and chemically deficient segregated grout characterized as moisture-rich and low cement content material with high concentrations of sulfate and alkali ions [15–17]. The accumulation of sulfate ions were apparently manifested by the grout segregation process that occurred soon after grout placement due to the ionic mobility of the sulfate ion that originated from the original grout material [16]. These issues have proven the importance of having good grout quality to extend the service life of bonded post-tensioned tendons. The extent of grout deficiency, moisture presence, aggressive ion accumulation, and grout pore water carbonation contribute to the severity of the defect.

Grout material testing for corrosion mitigation and quality control typically focus on minimizing the formation of bleed water that have been largely associated with the premature corrosion of strand. Specified testing included the wick-induced bleed tests, Schupak pressure test, and incline tube test. Building specifications also limit the chloride content, often prescribed as a percent of chloride per cement content. Various testing approaches for the corrosion of steel in the cementitious materials have been considered [18–24]. Trejo et al., 2009 [21], evaluated accelerated corrosion test procedures including the mini-macrocell test. An anodic potentiostatic polarization test was developed in consideration of chloride penetration through damaged tendon ducts as part of a Federal Highway Administration (FHWA) research project on the durability of bonded tendons in post-tensioned bridge structures [25]. The FHWA post-tensioning tendon installation and grouting manual [26] continues to refer to this test method. Schokker, 1999 [27], and Hamilton et al., 2000 [28], further developed the test method and addressed complications with the electrochemical polarization test parameters. Pacheco et al., 2006 [29], included the linear polarization resistance method to provide more practical testing than the anodic potentiostatic tests. Based on the research by Schokker and Hamilton, the post-tensioning institute (PTI) made provisions in the PTI M55 specification for grouting of post-tensioned structures for an accelerated corrosion test (ACT) for the assessment of grout materials [30]. The ACT gives provision for the acceptance of grout materials that exhibit a polarization resistance corresponding to a value greater than 700 $k\Omega \cdot cm^2$. The polarization resistance of steel embedded in the test grout material gives an indication as to if the grout constituent materials allow depassivation of the steel to occur. Further provisions allow alternative acceptance requirements by testing by an anodic potentiostatic polarization method for the grouted specimen immersed in chloride solution and polarized to +200 mV_{SCE} where the time to corrosion must exceed that of a control neat grout. The polarization would allow migration of the chloride ion through the grout and holds the steel at a large anodic polarization that would allow the fast detection of corrosion once chloride-induced corrosion initiates. Current specifications in Florida and Virginia require prepackaged grout materials to be tested according to the PTI ACT method whereby materials that exhibit a time to corrosion exceeding 1000 h are considered satisfactory. As mentioned earlier, this test component derived from the viewpoint of the ability of the grout to resist chloride penetration through the grout, as can occur in scenarios where there is incomplete protection provided by the tendon duct and reinforced concrete structural element but which does not directly address developed grout deficiencies such as segregation.

The rapid-macrocell test was developed under the strategic highway research program (SHRP) [31] for testing of the corrosion of steel rebar [32,33], including in standard specifica-

tions for testing of stainless steel rebar in ASTM A955 Annex 2.28. The rapid macrocell test has also been used in research for steel strand in grouts [34,35]. The test method separates two test cells, each comprising a steel electrode embedded in cementitious material or immersed in a representative test solution. The two test cells are electrically coupled with a connection wire and a shunt resistor and ionically coupled via a salt bridge (such as agar admixed with salt). Each test cell develops net anodic behavior or net cathodic behavior after its galvanic coupling where a net macrocell current between the cells can develop. With these test conditions controlled, the rapid-macrocell test can be used to differentiate corrosion conditions with small test elements and basic electronic instrumentation. In order to assess deficient grouts, the anode component should maintain grout material characteristics that allow for corrosion initiation such as pH, chloride concentration, sulfate concentration, etc. [36,37].

Due to the corrosion tendon failures in a Florida bridge in 2011 [8] associated with a prepackaged thixotropic grout that had developed material segregation, it was of interest to identify corrosion testing methods that would account for the susceptibility of grout materials to form physical and chemical deficiencies. It would be suggested that testing attuned to grout segregation (such as to identify grout robustness and corrosion mitigation) could be used to prescribe grouts resistant to aberrations in construction and provide greater confidence in material selection [38–41]. Full scale tendon mockups such as those required prior to bridge construction in Virginia for grout material selection may be cost prohibitive and excessive. Tests such as a modified incline tube test were used in research to identify grout segregation but this testing can also be costly. Furthermore, the chemistry of complex grout mix designs can be affected by the many environmental and construction factors including temperature, grout storage, pre-hydration, excess moisture mixing, etc. As construction can sometimes have delays in grout casting as well as other non-ideal construction conditions, specified grouts that are robust after adverse mixing and grouting conditions can minimize the severity of developed grout defects.

On a related technical note, inhibitor impregnation utilizing a silicon hydrocarbon polymer that forms a protective film was applied on tendons in a FDOT bridge (Jacksonville, FL, USA). Field results showed that inhibitor, as part of a commercially-available system, could be distributed along the length of the tendon via the strand interstitial spaces. The result of laboratory trials showed that the inhibitor-impregnated specimens had reduced corrosion by more than 90% comparing to untreated samples [42]. The procedure has since been used on PT tendons at risk of corrosion on other bridges, buildings, and industrial structures in Florida, Virginia, New York, Ontario, Newfoundland, and the UK. The field case study also showed severe corrosion of galvanized steel components in the presence of deficient grout [43,44]. The development of an accelerated corrosion test that considers the robustness of grout materials in terms of corrosion durability ideally could disseminate the beneficial effects of corrosion mitigation technologies such as the inhibitor impregnation as well as performance of other metallic component such as galvanized steel.

In this paper, the development of an accelerated material test that has been lacking in material specifications is described to identify materials that can be susceptible to segregation where the differentiation of localized grout chemistry could allow corrosion initiation. The outcome of the work would ideally provide information on the modality of tendon degradation (different from conventional PT corrosion mechanisms) in the presence of physically- and chemically-deficient grout and provide support for more discerning material specifications. The objective of the work presented here, as part of a larger test program, included to (1) to characterize the development of physical and chemical grout deficiencies due to excess mix water and water volume displacement, (2) to develop small scale test methodologies that identify deficient grout, and (3) to develop test methodologies to identify steel corrosion in deficient grout. To address these research goals, testing included methods that would promote the development of grout deficiencies. This included adverse mix conditions such as overwatering and grout pre-hydration for the grouts in vertically-deviated setups to promote water displacement. The results

presented here for commercially available grouts do not represent material performance as intended following accepted mixing protocols and specifications but were used rather for illustrative purposes to develop corrosion testing protocols that can address grout physical and chemical deficiencies.

2. Materials and Methods

Four grout products and a neat grout were used. Table 1 lists its chemical makeup determined by X-ray fluorescence testing. From previous research, it was identified that deficient grout can form at the upper elevation of vertically-deviated tendons due to the displacement of water-rich materials during the pumping stage of the grout installation. Table 2 details the conditions for grout material specimens. A replication of test specimens for each material condition is shown in Table 2. An excess of mix water, 10% above the manufacturers' recommended limit, was added. Previous research [14] used up to 15% excess water to create adverse conditions in attempts to reproduce the grout deficiencies in the field. However, the research here sought to provide fewer extreme conditions for practical implementation of testing to real world conditions but was aggressive enough to assess grout robustness with the earlier noted caveats.

Table 1. Grout chemical makeup analyzed by XRF.

Mass (%)	Grout A	Grout B	Grout C	Grout D	Neat Grout
Sodium (Na)	-	-	0.3, 0.3	0.03, -	-
Potassium (K)	0.3, 0.6	0, 0.01	1.1, 1.2	0.1, 0.1	0.2, 0.4
Calcium (Ca)	24.3, 45.1	30.5, 42.2	42.3, 46.5	33.9, 36.2	31.7, 47.6
Silicon (Si)	3.5, 6.6	4.3, 5.4	14.4,16.4	4.1, 4.2	4.1, 5.8
Sulfur (S)	0.6, 0.8	0.5, 0.7	1.5, 1.8	1.0, 1.1	0.6, 1.6
Chloride (Cl)	-	-	-	-	-

Table 2. INT and MIT grout material specimens.

Test Setup	Material	Number of Samples	Grout Condition
INT	Grout A	2	As Received and 10% extra mix water
	Grout B	2	As Received and 10% extra mix water
	Grout C	2	As Received and 10% extra mix water
		2	Expired and 10% extra mix water
	Grout D	2	Expired and 10% extra mix water
	Neat Grout	2	0.45 w/c
MIT	Grout A	6	As Received and 10% extra mix water
	Grout B	6	As Received and 10% extra mix water

Grout A was used for horizontal PT applications and Grout B was used for vertical applications.

The inverted T-test (INT) was proposed where a dramatic change in the vertical axial cross-section of the test specimen was introduced, allowing for localized accumulation of deficient grout materials. For example, if grout segregation were to occur in a 1 mm layer at the widest area of the Tee body, an equivalent volume of that material transported to the upper levels of the Tee header would be 2.89 cm in height. A schematic of the INT is shown in Figure 1. INT testing is benchtop in scale and significantly reduces material wastage and fabrication costs compared to MIT and full-scale mockup testing; however, the grout placement and dimensions are not representative of field grout pumping conditions. INT specimens were cast without (Figure 1a) and with steel (Figure 1b) for grout material and corrosion testing, respectively. The grout was mixed using an electric mixer and filled in the

mold by a manual pump. After 28 days of curing within the INT mold, sections of the mold were made for the material and corrosion testing. For material testing, the tee header was partitioned into three sections [0"–2", 12"–14", 24"–28", (0–5.1, 30.5–35.6, 61–71.1 cm)]. For corrosion testing, the tee header was partitioned into 9-inch length sections. The segments were cut and demolded. A 1/8-inch (3.2 mm) hole was drilled at the top of the exposed steel cross-section of each specimen and a steel screw was inserted so that a hard electrical contact was made. Insulted copper wire was soldered to the steel stud. Both the top and bottom of each specimen were coated with an epoxy to mask the exposed steel bar cross-section and the electrical connection.

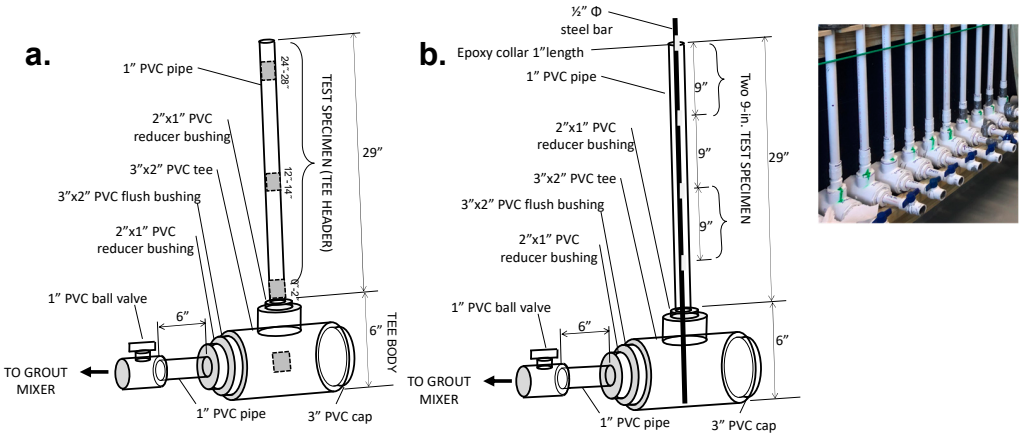

Figure 1. INT–test schematic: (**a**) grout material testing and (**b**) corrosion testing.

MIT testing is based on the incline-tube test which was previously developed by industry groups to assess grout durability and includes dimensions and grout placement methods better representative of actual construction. Based on positive research outcomes to identify grout segregation in previous research, the MIT was revisited. Grout A and B with 10% excess water were cast according to Florida Standard Specification Section 938. The test setup generally consists of pumping grout in a 3-inch (7.6 cm) diameter pipe, along a 15-foot (4.6 m) length at a 30 degree incline. A schematic of the specimen assembly used in this research is shown in Figure 2. Testing was conducted in ambient South Florida outdoor conditions. A 15-foot (4.6 m) 0.5-inch (1.3 cm) diameter steel bar was placed in the MIT for additional corrosion testing. A manual grout pump was used to inject the grout into the MIT assembly. After ~365 days of hydration, for the corrosion testing, at the base of each tendon, the embedded steel bar was exposed for electrical contact for the electrochemical testing. Six portals [4 × 3 inch (10.2 × 7.6 cm)]) along the length of the MIT specimen were made to expose the grout within the duct by cutting and removing the PVC cover. Grout was sampled from each of the MIT specimens within the top and bottom 6 inches of the duct.

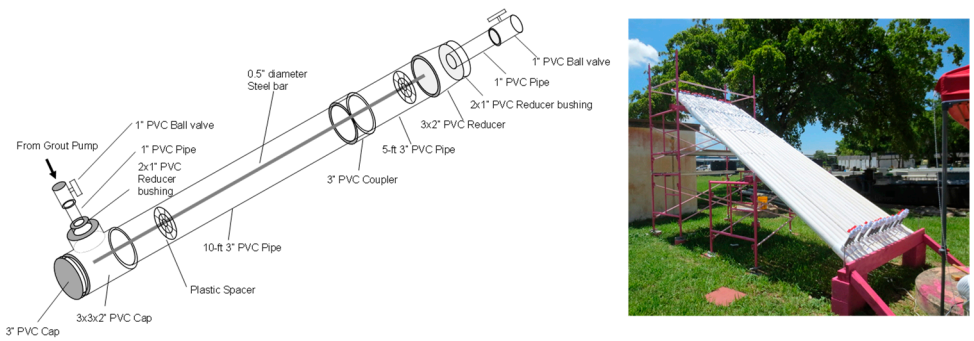

Figure 2. MIT–test set up. **Left**: tendon schematic. **Right**: outdoor test setup.

The INT test segments were placed in saturated calcium hydroxide solution (pH 12.6) made from deionized water. A stainless steel rod, placed adjacent to the test segment in the test solution, was used as a counter electrode. A saturated calomel electrode (SCE) was used as a reference electrode. For the MIT test setup, at the base of each tendon, the embedded steel bar was exposed so that electrical contact can be made for the electrochemical testing. A counter electrode made out of activated titanium mesh (4 × 3 inch) inserted between two wet sponges was affixed to exposed grout surface at openings made in the duct. A pen copper/copper-sulfate reference electrode (CSE) was placed at the center of the fixture.

The open-circuit potential (OCP) and linear polarization resistance (LPR) measurements were made using an SCE (for INT specimens) and CSE (for MIT specimens). The LPR testing was made from the OCP and a cathodicaly polarized 25 mV at 0.05 or 0.1 mV/s scan rate. Electrochemical impedance spectroscopy (EIS) was conducted at the OCP condition using a 10 mV AC perturbation in the frequency range of 100 kHz to 1 kHz, sampling 10 data points per decade. The solution resistance, Rs, was determined as the high frequency limit by fitting the impedance spectrum to the Randles equivalent circuit analog and was used to correct for the measured polarization resistance by LPR (Rp') following the equation $Rp = Rp' - Rs$.

3. Results and Discussion

3.1. Material Characteristic

The INT specimens allowed for the physical separation of grout materials from the tee header and tee body. The results of the moisture content are shown in Figure 3. There was strong differentiation in moisture content between the tee header and body for Grout C and expired Grout C and D. Grouts C and D appeared to have higher contents of fine materials such as silica- and calcium-bearing components that may have contributions to the physical separation of material. Pre-hydration of the material may also allow development of non-binding filler components that may be susceptible to differential transport. Differences in moisture content of the grout from the tee header and body were less apparent for Grouts A and B.

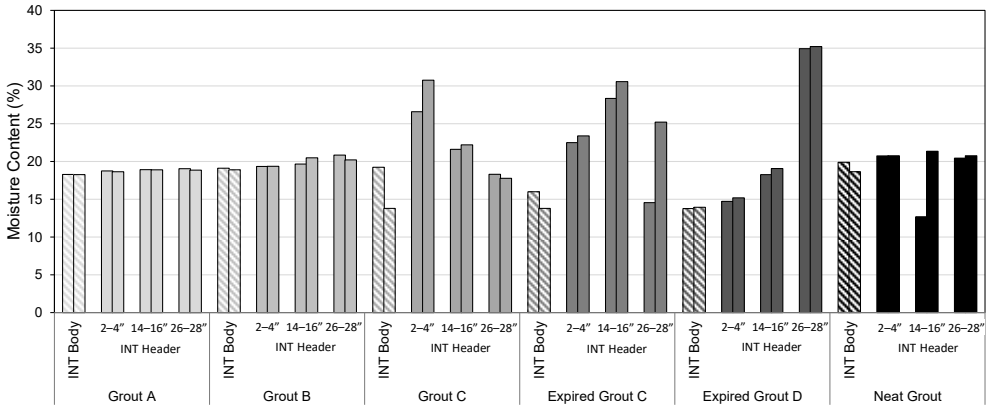

Figure 3. Moisture content of grout cast in INT with 10% extra mix water. Values for grout in the tee body and at various elevations of the tee header given.

The grout from the INT and MIT specimens was further tested following the updated FM 5-618 method [45] to assess the effects of poor construction on the extent to which sulfate ions can accumulate including overwatering and prehydration (Figure 4). Different grout products had different yields of leached sulfate ions in the INT header. As shown in Figure 4, higher sulfate levels (apparently already dissolved in the pore water) were generally observed in the tee header than the tee body, likely relating to the displacement of water to the top of the specimen. Comparisons of the average sulfate concentrations in MIT specimens do indicate differentiation of the sulfate content in the grout from the upper and lower elevations of the ducts. For both Grout A and B, the average sulfate content

in the grout from the top of the specimen was higher than the average sulfate content from the bottom of the specimen. It was anticipated that MIT testing of the other grout materials would produce differentiation in sulfate content between the top and bottom elevations as well.

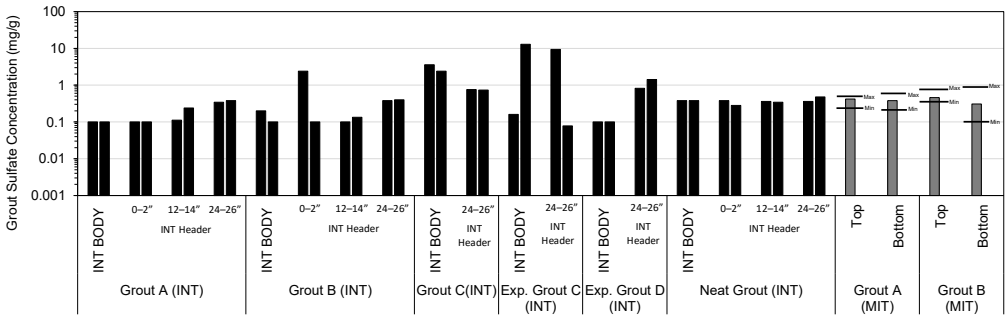

Figure 4. Comparison of sulfate ion concentrations in grout from INT and MIT. Values for grout in the tee body and at various elevations of the tee header given.

3.2. Electrochemical Characteristic

As shown in Figures 5 and 6, the steel embedded in Grout A and B all developed passive potentials in the range of $-100 < OCP < -200$ mV_{SCE}. Some of the specimens cast with neat grout developed similar passive potentials. However, specimens cast with Grout C and expired Grout C and D developed more electronegative potentials at levels that may be interpreted as active corrosion (as negative as -450 mV_{SCE}) according to ASTM C876 [46]. This observation was coincident with the physical grout deficiencies described earlier [47]; however, since the specimens were immersed in saturated calcium hydroxide solution prior to testing and were tested in chloride-free saturate calcium hydroxide solution, corrosion activation was not expected. Testing of the grout pore water for chemical deficiencies (Figure 4) showed higher sulfate accumulation in Grout C and expired grout C and D.

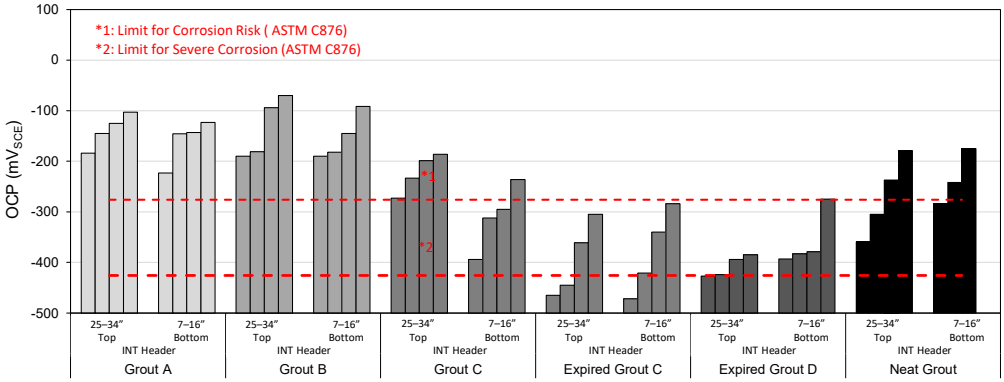

Figure 5. Open–circuit potential for INT testing. Values for grout at various elevations of the tee header given.

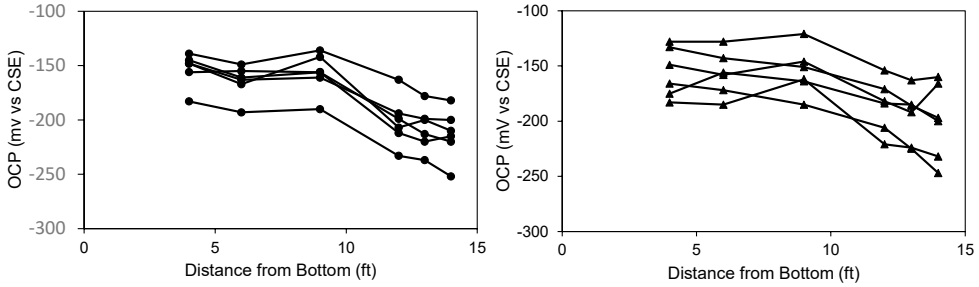

Figure 6. Open–circuit potential of steel in MIT specimens. **Left**: Grout A. **Right**: Grout B.

Consistent with the OCP measurements, the specimens cast with Grout C and expired grout C and D had much lower Rp (Figure 7). The OCP for the steel in the MIT specimens is shown in Figure 6. The OCP of the steel showed a modest decrease to more electronegative potentials at the upper 5 feet (1.5 m) of the tendons. However, the potentials overall were generally indicative of passive conditions. Indeed, the resolved Rp shown in Figure 7 did not show strong indication for elevated corrosion rates for the steel at the upper elevations. The greater corrosion activity of steel in the grout with elevated sulfate concentrations was due to the ability of sulfate ions that are made present at the steel surface early on in the grout placement to destabilize the passive oxide film. The sulfate ions may be able to adsorb onto the steel surface and compete with favorable oxides and hydroxides to hinder the development of the passive film [48–52].

Figure 8 shows the resolved solution resistance for both INT and MIT setups. Generally, the specimens showed similar solution resistance except for Grout C which showed the highest solution resistance. For the MIT specimens, the resolved solution resistance of the grout, however, was generally differentiated between locations from the top and bottom of the tendon, indicating differentiation in the grout and moisture content by elevation (Figure 8). The lower solution resistance in the deficient grout that develops at higher elevations would allow more efficient coupling of local anodes and steel cathodes to support greater corrosion activity. The lower solution resistance was resolved for grout at the top of the tendon than at the lower elevations, further supporting the use of the MIT as a means to test grout performance. It was noted that greater differentiation in solution resistance between tendon elevations as well as lower values were obtained for Grout A compared to Grout B. Indeed, Grout B had better performance as it was designed for vertical PT applications and Grout A has been accepted for only horizontal PT applications. The sulfate content in Grout B was better differentiated between the high point elevation (~0.48 mg/g) and the low point elevation (~0.13 mg/g) than for Grout A but Grout A showed as much as ~0.6 mg/g sulfate at high and low point elevations.

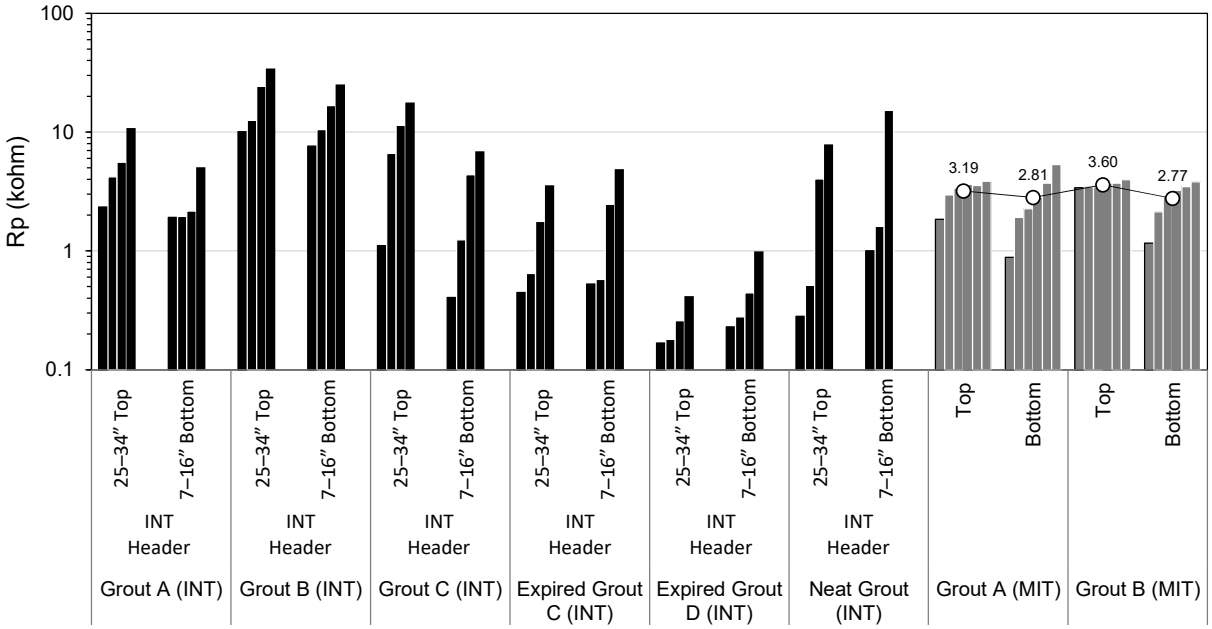

Figure 7. Measured polarization resistance grout from MIT and INT specimens. Values for grout at various elevations of the INT tee header or MIT duct location given.

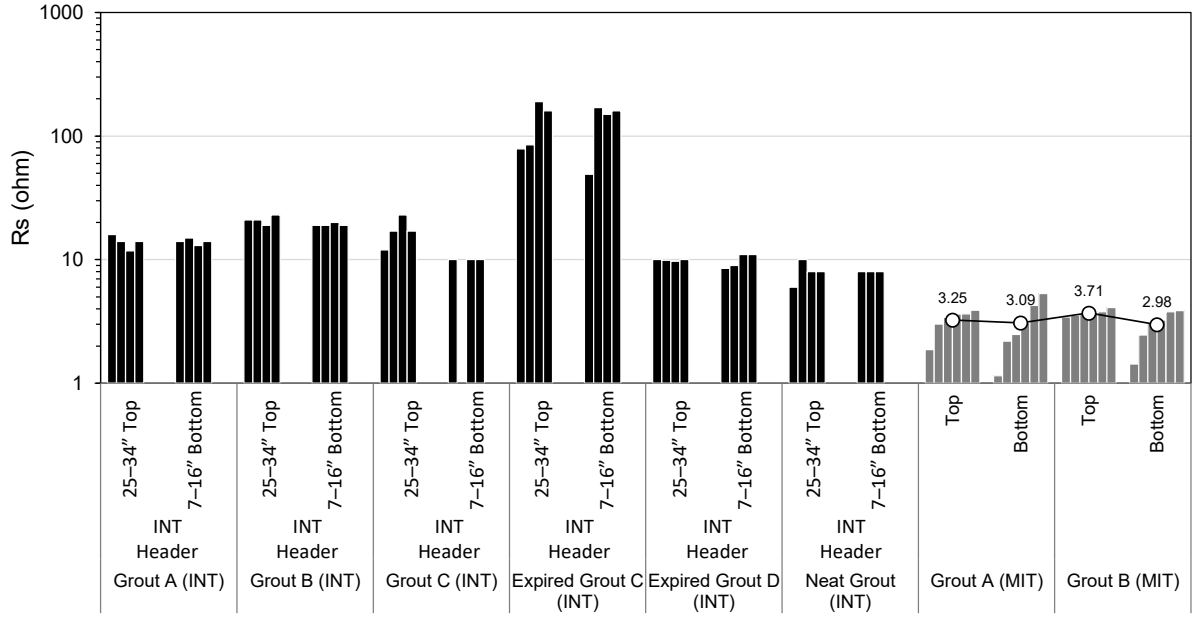

Figure 8. Solution resistance of grout from MIT and INT specimens. Values for grout at various elevations of the INT tee header or MIT duct location given.

3.3. Risk Assessment Based on the Sulfate Limit

The corrosion potentials and corrosion current densities for the steel embedded in the MIT specimens and the INT specimens show general correlation to the grout sulfate content (Figures 9 and 10). As shown in Figure 9, the corrosion potential decreases to more electronegative values at the higher sulfate concentrations. Likewise, the corrosion current density showed a general increasing trend with the higher sulfate levels and indications for some critical threshold value with elevated rates above a sulfate concentration for deficient grouts with characteristic pH and electrical resistance (Figure 10). The values produced from the test program here were consistent with historical data from earlier research [8,14,17,36,48] where an estimated critical sulfate concentration of 0.7 mg/g was observed (where the OCP was <-300 mV_{CSE} and $i_{corr} > 0.1$ $\mu A/cm^2$ [48]), further verifying the adverse effects of elevated sulfate ion concentrations in the segregated grout.

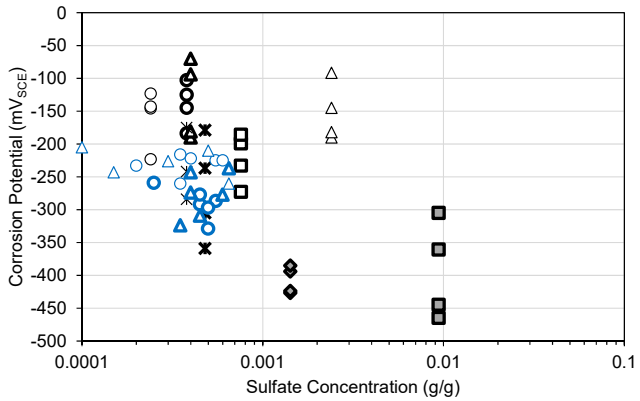

Figure 9. Correlation of steel corrosion potential and grout sulfate content. Circle: Grout A. Triangle: Grout B. Square: Grout C. Diamond: Grout D. Cross: Neat Grout. Filled: Expired Grout. Blue: MIT. Black: INT.

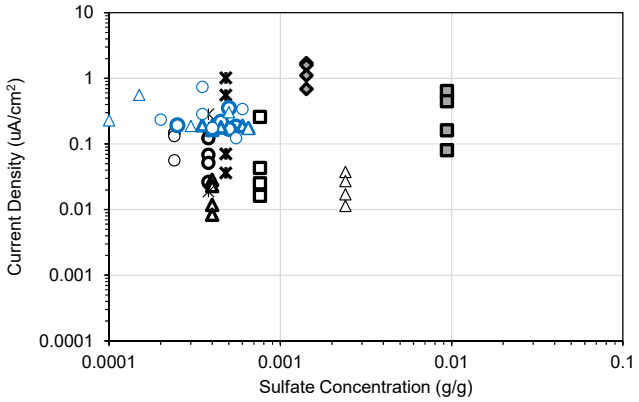

Figure 10. Correlation of steel corrosion current density and grout sulfate content. Circle: Grout A. Triangle: Grout B. Square: Grout C. Diamond: Grout D. Cross: Neat Grout. Filled: Expired Grout. Blue: MIT. Black: INT.

The data in Figures 9 and 10 show that there is differentiation in the corrosion behavior of steel in grout materials that develop different chemistries in its pore water. The expired grouts developed the highest sulfate ion concentrations and showed the greatest susceptibility for corrosion development. The aggressive chemistries were developed in expired Grouts C and D subjected to water transport associated with vertical deviations such that transport can be gaged by the grout that accumulate in the vertical tee header in the INT test. The most electronegative potentials and greatest corrosion rates of steel developed in specimens from the INT tee header coincident with the highest sulfate ion concentrations. Although not as sharply parced here with testing of Grout A and B, MIT specimens in other research [14,15] have shown similar discrimination for susceptible grout materials. The results imply that the simple INT test setup can be useful to identify grout segregation robustness. Testing with greater degrees of grout pre-hydration and added water levels may be considered in future research, including the possibility to identify threshold levels for various grout materials, but this was not within the scope of the work for the practical evaluation of grout robustness for material acceptance.

The results of the testing further indicate that testing for corrosion in field structures should include grout sampling in vertically-deviated regions of PT tendons (such as deviators, joints, and anchors) where water-rich deficient grout materials can accumulate. The testing can include the quality of grout hydration, moisture content, electrical resistance, and sulfate ion content as well as conventional testing for voids, bleed, and chloride ion content.

4. Conclusions

It was shown that the different grout products have widely different propensities for the segregation and accumulation of sulfate ions but that adverse grout mixing practices such as the addition of 10% mix water above the manufacturer's recommendation and pre-hydration promoted the development of grout deficiencies, including the accumulation of sulfate ions, even without external sulfate ion sources.

The corrosion potentials and corrosion current densities for the steel embedded in the INT and MIT specimens were correlated with the grout sulfate content and the values produced from the test program here were consistent with historical data from earlier research, further verifying the adverse effects of elevated sulfate ion concentrations in the segregated grout. The expired grouts developed the highest sulfate ion concentrations and showed the greatest susceptibility for corrosion development. The sulfate limits expressed as mass relative to the grout sample mass can be implemented to normalize the leaching volume and mass size.

The sulfate content associated with severe corrosion was associated with deficient grout materials with a high moisture content. As such, it is recommended that the sulfate

testing is incorporated into material testing to assess the susceptibility of grout materials to segregate. Test methods such as the modified incline tube test incorporating overwatering in the grout mixing or alternative testing to facilitate the capturing of displaced water, such as the inverted-tee test, should be considered for grout material sampling. In the field, the extraction of grout materials from locations typically associated with moisture and/or bleeding such as at high points, points of deviation, and joints should be considered.

Author Contributions: Writing—review and editing, S.P. and K.L.; Supervision, K.L. All authors have read and agreed to the published version of the manuscript.

Funding: This research was funded by Florida Department of Transportation (FDOT), grant number BDV29-977-44.

Data Availability Statement: All data contained within the article.

Acknowledgments: This investigation was supported by the Florida Department of Transportation (FDOT). The opinions, findings, and conclusions expressed here are those of the authors and not necessarily those of the FDOT or the US Department of Transportation.

Conflicts of Interest: The authors declare no conflict of interest.

References

1. Hurst, M.K. *Prestressed Concrete Design*; CRC Press: Boca Raton, FL, USA, 2017.
2. Hewson, N.R. *Prestressed Concrete Bridges: Design and Construction*; Thomas Telford Publishing: London, UK, 2003.
3. Lau, K.; Permeh, S.; Lasa, I. Corrosion of prestress and posttension reinforced concrete bridges. In *Corrosion of Steel in Concrete Structures*, 2nd ed.; Poursaee, A., Ed.; Woodhead Publishing: Cambridge, UK, 2023; pp. 81–105. [CrossRef]
4. Powers, R.G. *Corrosion Evaluation of Post-Tensioned Tendons on the Niles Channel Bridge*; Florida Department of Transportation: Tallahassee, FL, USA, 1999.
5. Corven Engineering. *Mid-Bay Bridge Post-Tensioning Evaluation*; Final Report to Florida Department of Transportation; Florida Department of Transportation: Tallahassee, FL, USA, 2001.
6. Hartt, W.; Venugopalan, S. *Corrosion Evaluation of Post-Tensioned Tendons on the Mid Bay Bridge in Destin, Florida*; Final Report; Florida Department of Transportation: Tallahasse, FL, USA, 2002.
7. Hansen, B. Forensic Engineering: Tendon Failure Raises Questions about Grout in Post-Tensioned Bridges. *Civ. Eng. News* **2007**, *77*, 17–18.
8. Lau, K.; Lasa, I.; Paredes, M. *Corrosion Development of PT Tendons with Deficient Grout: Corrosion Failure in Ringling Causeway Bridge*; Draft Report; Florida Department of Transportation State Materials Office: Gainesville, FL, USA, 2011.
9. Lau, K.; Powers, R.; Paredes, M. Corrosion Evaluation of Repair-Grouted Post-Tensioned Tendons in Presence of Bleed Water. In Proceedings of the CORROSION 2013, Orlando, FL, USA, 17–21 March 2013; NACE International: Houston, TX, USA, 2013.
10. Lau, K.; Rafols, J.; Paredes, M.; Lasa, I. Laboratory Corrosion Assessment of Post-Tensioned Tendons Repaired with Dissimilar Grout. In Proceedings of the CORROSION 2013, Orlando, FL, USA, 17–21 March 2013; NACE International: Houston, TX, USA, 2013.
11. Lau, K.; Paredes, M.; Lasa, I. Corrosion Failure of Post-Tensioned Tendons in Presence of Deficient Grout. In Proceedings of the CORROSION 2013, Orlando, FL, USA, 17–21 March 2013; NACE International: Houston, TX, USA, 2013.
12. Lau, K.; Lasa, I.; Paredes, M. Bridge tendon failures in the presence of deficient grout. *Mater. Perform.* **2013**, *52*, 64–68.
13. Lau, K.; Lasa, I.; Paredes, M. Update on Corrosion of Post-Tensioned Tendons with Deficient Grout. In Proceedings of the CORROSION 2014, San Antonio, TX, USA, 9–13 March 2014; NACE International: Houston, TX, USA, 2014.
14. Permeh, S.; Krishna Vigneshwaran, K.K.; Lau, K. *Corrosion of Post-Tensioned Tendons with Deficient Grout*; Final Report to Florida Department of Transportation, Contract No. BDV29-977-04; Florida Department of Transportation: Tallahassee, FL, USA, 2016.
15. Permeh, S.; Lau, K.; Tansel, B. Moisture and ion mobilization and stratification in post-tensioned (PT) grout during hydration. *Case Stud. Constr. Mater.* **2021**, *15*, e00644. [CrossRef]
16. Permeh, S.; Krishna Vigneshwaran, K.K.; Lau, K.; Lasa, I.; Paredes, M. Material and Corrosion Evaluation of Deficient PT Grout with Enhanced Sulfate Concentrations. In Proceedings of the CORROSION 2015, Dallas, TX, USA, 15–19 March 2015; NACE International: Houston, TX, USA, 2015.
17. Permeh, S.; Krishna Vigneshwaran, K.K.; Echeverría, M.; Lau, K.; Lasa, I. Corrosion of Post-Tensioned Tendons with Deficient Grout, Part 2: Segregated Grout with Elevated Sulfate Content. *Corrosion* **2018**, *74*, 457–467. [CrossRef] [PubMed]
18. *ASTM G109*; Standard Test Method for Determining Effect of Chemical Admixtures on Corrosion of Embedded Steel Reinforcement in Concrete Exposed to Chloride Environments. ASTM: West Conshohocken, PA, USA, 2013.
19. *ASTM A955*; Standard Specification for Deformed and Plain Stainless-Steel Bars for Concrete Reinforcement. ASTM: West Conshohocken, PA, USA, 2019.

20. Palumbo, N. Accelerated Corrosion Testing of Steel Reinforcement in Concrete. Master's Thesis, McGill University Libraries, Montreal, QC, Canada, 1991.
21. Trejo, D.; Halmen, C.; Reinschmidt, K. *Corrosion Performance Tests for Reinforcing Steel in Concrete*; Technical report (No. FHWA/TX-09/0-4825-1); Texas Transportation Institute: Bryan, TX, USA, 2009.
22. Deb, S. *Accelerated Short-Term Techniques to Evaluate Corrosion in Reinforced Concrete Structures*; The Master Builder: Southampton, UK, 2012; pp. 248–255.
23. Ožbolt, J.; Sola, E.; Balabanić, G. Accelerated Corrosion of Steel Reinforcement in Concrete: Experimental Tests and Numerical 3D FE Analysis. In Proceedings of the CONCREEP 10, Vienna, Austria, 21–23 September 2015; pp. 108–117.
24. Permeh, S.; Lau, K. Review of Electrochemical Testing to Assess Corrosion of Post-Tensioned Tendons with Segregated Grout. *Constr. Mater.* **2022**, *2*, 70–84. [CrossRef]
25. Thompson, N.G.; Lankard, D.R.; Sprinkel, M.M. *Improved Grouts for Bonded Tendons in Post-Tensioned Bridge Structures*; FHWA-RD-91-092, Cortest Columbus Technologies; Federal Highway Administration: Washington, DC, USA, 1992.
26. Corven, J. *Post-Tensioning Tendon Installation and Grouting Manual*; FHWA-NHI-13-026; Federal Highway Administration: Washington, DC, USA, 2013.
27. Schokker, A.J. Improving Corrosion Resistance of Post Tensioned Substructures Emphasizing High Performance Grouts. Ph.D. Thesis, The University of Texas at Austin, Austin, TX, USA, 1999.
28. Hamilton, H.R.; Wheat, H.G.; Breen, J.E.; Frank, K.H. Corrosion testing of grout for posttensioning ducts and stay cables. *J. Struct. Eng.* **2000**, *126*, 163–170. [CrossRef]
29. Pacheco, A.R.; Schokker, A.J.; Hamilton, H.R. *Development of a Standard Accelerated Corrosion Test for Acceptance of Post-Tensioning Grouts in Florida*; Final Report, Contract No. 00026900; Florida Department of Transportation: Tallahassee, FL, USA, 2006.
30. *PTI M55.1-12*; Specification for Grouting of Post-Tensioned Structures. Post Tensioning Institute: Farmington Hills, MI, USA, 2013.
31. Martinez, S.; Darwin, D.; Steven, L.; McCabe, S.L.; Locke, C.E., Jr. *Rapid Test for Corrosion Effects of Deicing Chemicals in Reinforced Concrete*; University of Kansas Center for Research, Inc.: Lawrence, KS, USA, 1990.
32. Darwin, D.; Browning, J.; O'Reilly, M.; Locke, C.E.; Virmani, Y.P. *Multiple Corrosion Protection Systems for Reinforced Concrete Bridge Components*; University of Kansas: Lawrence, KS, USA, 2007.
33. Darwin, D.; Strurgeon, W. *Rapid Macrocell Tests of Enduramet Steel Bars*; The University of Kansas Center for Research, Inc.: Lawrence, KS, USA, 2011.
34. O'Reilly, M.; Darwin, D.; Browning, J. *Corrosion Performance of Prestressing Strands in Contact with Dissimilar Grouts, (No. KS-12-4)*; Kansas. Dept. of Transportation: Topeka, KS, USA, 2013.
35. O'Reilly, M.; Darwin, D.; Browning, J. Corrosion Performance of Prestressing Strands in Contact with Dissimilar Grouts. *ACI Mater. J.* **2015**, *112*, 491–500. [CrossRef]
36. Krishna Vigneshwaran, K.K.; Permeh, S.; Echeverría, M.; Lau, K.; Lasa, I. Corrosion of Post-Tensioned Tendons with Deficient Grout, Part 1: Electrochemical Behavior of Steel in Alkaline Sulfate Solutions. *Corrosion* **2018**, *74*, 362–371. [CrossRef] [PubMed]
37. Permeh, S.; Lau, K. Localized corrosion of steel in alkaline solution with low-level chloride and elevated sulfate concentrations. *Cement* **2022**, *10*, 100051. [CrossRef]
38. Sonawane, R.; Permeh, S.; Garber, D.; Lau, K.; Simmons, R.; Duncan, M. Test Methods to Identify Robustness of Grout Materials to Resist Corrosion. In *Proceedings of the CORROSION 2020, Digital Proceedings*; NACE International: Houston, TX, USA, 2020.
39. Permeh, S.; Sonawane, R.; Lau, K.; Duncan, M.; Simmons, R. Update on the Evaluation of Grout Robustness and Corrosion by Accelerated Corrosion and Rapid Macrocell Testing. In Proceedings of the CORROSION 2021, Virtual Conference, 19–30 April 2021; NACE International: Houston, TX, USA, 2021.
40. Permeh, S.; Lau, K.; Tansel, B. *Development of Standard Methodology to Measure Sulfate Ions in Post-Tensioned Grouts*; Final Report to Florida Department of Transportation, Contract No. BDV29-977-43; Florida Department of Transportation: Tallahassee, FL, USA, 2021.
41. Permeh, S.; Lau, K.; Matthew, D. Accelerated Testing to Assess Robustness of Post-Tensioning Grout. *Mater. Perform.* **2021**, *60*, 34–38.
42. Whitmore, D.; Tore Arnesen, P.E. Evaluation and Mitigation of Post-Tensioned Steel Corrosion. In *Eighth Congress on Forensic Engineering*; ASCE: Reston, VA, USA, 2020.
43. Permeh, S.; Lau, K. Corrosion of galvanized steel in alkaline solution associated with sulfate and chloride ions. *Constr. Build. Mater.* **2023**, *392*, 131889. [CrossRef]
44. Bonilla, A.; Argiz, C.; Moragues, A.; Gálvez, J.C. Effect of Sulfate Ions on Galvanized Post-Tensioned Steel Corrosion in Alkaline Solutions and the Interaction with Other Ions. *Materials* **2022**, *15*, 3950. [CrossRef] [PubMed]
45. *FM 5-618*; Florida Method of Test for Sampling of Post-Tensioned Tendon Grout. Florida Department of Transportation: Tallahassee, FL, USA, 2018.
46. *ASTM C876-15*; Standard Test Method for Corrosion Potentials of Uncoated Reinforcing Steel in Concrete. ASTM: West Conshohocken, PA, USA.
47. Permeh, S.; Lau, K. *Accelerated Corrosion Testing of Grouts for PT Steel Strand*; Final Report to Florida Department of Transportation, Contract No. BDV29-977-44; Florida Department of Transportation: Tallahassee, FL, USA, 2021.
48. Permeh, S.; Krishna Vigneshwaran, K.K.; Lau, K.; Lasa, I. Corrosion of Post-Tensioned Tendons with Deficient Grout, Part 3: Segregated Grout with Elevated Sulfate and Vestigial Chloride Content. *Corrosion* **2019**, *75*, 848–864. [CrossRef] [PubMed]

49. Permeh, S.; Lau, K.; Duncan, M.; Simmons, R. Identification of steel corrosion in alkaline sulfate solution by electrochemical noise. *Mater. Corros.* **2021**, *72*, 1456–1467. [CrossRef]
50. Sarab, D.F.; Permeh, S.; Lau, K. Effect of Early and Late Presence of Sulfate Ions on Steel Corrosion Development in Alkaline Solution. In Proceedings of the AMPP Annual Conference + Expo 2023, Denver, CO, USA, 19–23 March 2023.
51. Permeh, S.; Lau, K.; Duncan, M.; Simmons, R. Initiation of localized steel corrosion in alkaline sulfate solution. *Mater. Struct.* **2021**, *54*, 143. [CrossRef]
52. Chen, Z.; Wei, Z.; Chen, Y.; Nong, Y.; Yi, C. Molecular insight into iron corrosion induced by chloride and sulphate. *Comput. Mater. Sci.* **2022**, *209*, 111429. [CrossRef]